

Branching Fractions of B Meson Decays in Mesogenesis

Gilly Elor,^a Alfredo Walter Mario Guerrero^b

^a*PRISMA⁺ Cluster of Excellence & Mainz Institute for Theoretical Physics
Johannes Gutenberg University, 55099 Mainz, Germany*

^b*INFN, Sezione di Padova*

E-mail: gelor@uni-mainz.de, guerrera@pd.infn.it

ABSTRACT: Production of the matter-antimatter asymmetry in the B -Mesogenesis mechanism is directly related to the branching fraction of seemingly baryon number violating decays of B mesons into a light Standard Model baryon and missing energy. Achieving the observed baryon asymmetry requires that the branching fraction for such decays be greater than about $10^{-7} - 10^{-5}$. Experimental searches at B Factories and Hadron Colliders target specific decay modes. Therefore, computing the exclusive branching fraction for each decay is a critical step towards testing Mesogenesis. In this work we use QCD Light Cone Sum Rules to compute the form factors and branching fractions of the various possible channels contributing to the baryon asymmetry. Using the results, we comment on implications for current and future experimental searches.

Contents

1	Introduction	3
2	Overview of B-Mesogenesis	4
3	Form Factors from Light Cone Sum Rules	7
4	Results	9
4.1	Discussion of Results	9
4.2	Implications for Mesogenesis	12
5	Outlook	13
A	Technical Details	14
A.1	Form Factors from LCSR	14
A.2	Charmed Sector Distribution Amplitudes	15
A.3	BCL Fits and Parameters	16

1 Introduction

Under the standard paradigm of inflationary cosmology the Universe is born with equal parts matter and anti-matter. This necessitates a dynamical mechanism of *baryogenesis* to generate the asymmetry necessary to seed the complex structures observed today. The required primordial baryon asymmetry is inferred to be $Y_{\mathcal{B}}^{\text{meas}} \equiv (n_B - n_{\bar{B}})/s = (8.718 \pm 0.004) \times 10^{-11}$ from measurements of the Cosmic Microwave Background (CMB) [1, 2] and light element abundances after Big Bang Nucleosynthesis (BBN) [3]. Another outstanding mystery is the nature and origin of dark matter; the gravitationally inferred, but yet to be experimentally detected, component of matter which makes up roughly 26% of the energy of the Universe today [1, 2]. Recently proposed mechanisms of *Mesogenesis* [4–6] use Standard Model (SM) meson systems to generate both the baryon asymmetry and the dark matter abundance of the Universe.

Many mechanisms have been proposed since 1967 when Sakharov first introduced the conditions [7] necessary for baryogenesis; C and CP Violation (CPV), baryon number violation, and departure from thermal equilibrium. Traditional mechanisms of baryogenesis often involve high scales and massive particles leading to dismal prospects for experimental verification¹. In contrast, mechanisms of Mesogenesis generate the baryon asymmetry of the Universe by leveraging the CPV within SM meson systems. Excitingly, Mesogenesis is directly testable at hadron colliders and *B*-factories [9, 10], with additional indirect signals at Kaon and Hyperon factories [11, 12] and even upcoming neutrino experiments such as DUNE and Hyper-Kamiokande [13] (see also [8, 14–16] for summaries). A search for operator through which neutral *B*-Mesogenesis can proceed has already been conducted by the Belle-II collaboration [17], and a search has also been proposed at LHCb [18].

Production of the baryon asymmetry in the Neutral *B*-Mesogenesis mechanism [4] is directly related to the branching fraction of seemingly baryon number violating decays of neutral $B_{s,d}^0$ mesons into a light SM baryon and missing energy. Successful baryogenesis in this framework predicts this observable should be $\text{Br}(B_{s,d}^0 \rightarrow \mathcal{B}_{\text{SM}}^0 + \text{MET}) \gtrsim \mathcal{O}(10^{-5})$ to generate the observed baryon asymmetry [4, 9]. Charged *B* Mesogenesis [6], links the baryon asymmetry to the decays of the B^\pm mesons and requires $\text{Br}(B^\pm \rightarrow \mathcal{B}_{\text{SM}}^\pm + \text{MET}) \gtrsim \mathcal{O}(10^{-6})$. Furthermore, a measurement of the branching fraction as low as 10^{-7} could be an indication that a Mesogenesis mechanism is at play.

The nature of the final state SM baryon \mathcal{B}_{SM} in these decays depends on the flavor structure of the operator through which *B*-Mesogenesis proceeds (see Table 1 for a list of all the possible contributing decays). Experimental searches target *B* meson decay modes to specific final states, for instance the Belle-II collaboration set a limit on the branching fraction for B_d^0 decaying into a neutral Λ baryon and missing energy [17]. Therefore, the computation of the exclusive branching fractions of the various possible decay modes is critical for testing *B*-Mesogenesis. Searching for such *B* meson decays down to the $\text{Br} \sim 10^{-7}$ level will fully test the landscape of different Mesogenesis possibilities.

In this work we leverage the powerful machinery of QCD Light Cone Sum Rules (LC-SRs), first introduced in [19–21], reviewed in [22], to compute the branching fractions of the

¹See [8] for a summary of some interesting new ideas for testing traditional mechanisms.

various channels that could generate the baryon asymmetry. The hard scattering amplitude of the B meson to baryon transition is convoluted with the Distribution Amplitude (DA) of the baryon; these are fundamental non perturbative functions that can be interpreted as light-cone wave functions integrated over transverse quark momenta [23, 24]. Using our results, we comment on implications for current and future experimental searches in light of existing collider and flavor constraints on the model.

This paper is organized as follows: in Sec. 2 we first review the mechanism of B -Mesogenesis. We specifically emphasize the details most useful for an experimentalist eager to conduct such searches. Next, in Sec. 3, we detail the results of the LCSR's derivation of the form factors and branching fraction of the relevant B meson decays. Our main results are presented in Figure 2 and 3 and in Table 1, we further discuss the results and implications for Mesogenesis in Sec. 4. We conclude in Sec. 5 with an outlook on future directions. Appendices A.1, A.2, and A.3 contain supplementary details on the formalism and derivation.

2 Overview of B -Mesogenesis

Here we provide a brief review of the neutral B -Mesogenesis mechanism, with particular emphasis on the those ingredients most relevant for experimental searches.

The baryon asymmetry and dark matter abundance are produced through B -Mesogenesis as follows: we first assume the late time out of equilibrium production of equal numbers of $B_{s,d}^0$, $\bar{B}_{s,d}^0$ and B^\pm mesons² when the temperature of the Universe was $5 \text{ MeV} \lesssim T \lesssim 100 \text{ MeV}$ i.e. after the QCD phase transition but before BBN. The produced B mesons will then undergo SM CP violating processes before decaying into a dark sector state charged under SM baryon number and a SM baryon. The end result is an equal and opposite baryon asymmetry in the dark and the visible sector which is directly proportional to the branching fraction of the exotic decay of the B mesons. In the case of Neutral B -Mesogenesis [4], the generated asymmetry will also depend on the charge asymmetry of the $\bar{B}^0 - B^0$ oscillations, and indirectly on a host of other observables (see [9] for an overview). Achieving the observed baryon asymmetry [9], in light of current world averages limiting the CPV in the meson systems, requires an inclusive branching fraction $\text{Br}(B_{s,d}^0 \rightarrow \psi_{\mathcal{B}} + \mathcal{B}_{\text{SM}}) \gtrsim 10^{-5}$. Where $\psi_{\mathcal{B}}$ is a dark fermion carrying baryon number -1 , and \mathcal{B}_{SM} is a neutral SM baryon. Charged B Mesogenesis [6], leverages CPV in SM meson decays and requires $\text{Br}(B^+ \rightarrow \mathcal{B}_{\text{SM}}^+ + \psi_{\mathcal{B}}) \gtrsim \mathcal{O}(10^{-6})$ to generate the observed baryon asymmetry³. In both cases the exact nature of the SM baryon depends on the flavor structure of the UV model as will be discussed below. Indeed, various different decay modes can contribute to the generation of the baryon asymmetry.

²This can be achieved if a scalar field, perhaps related to inflation, comes to dominate the energy density of the Universe at late times.

³Note that fully verifying this *flavor* of Mesogenesis requires future generation experiments, and as such is less testable on shorter time scales than its neutral counterpart.

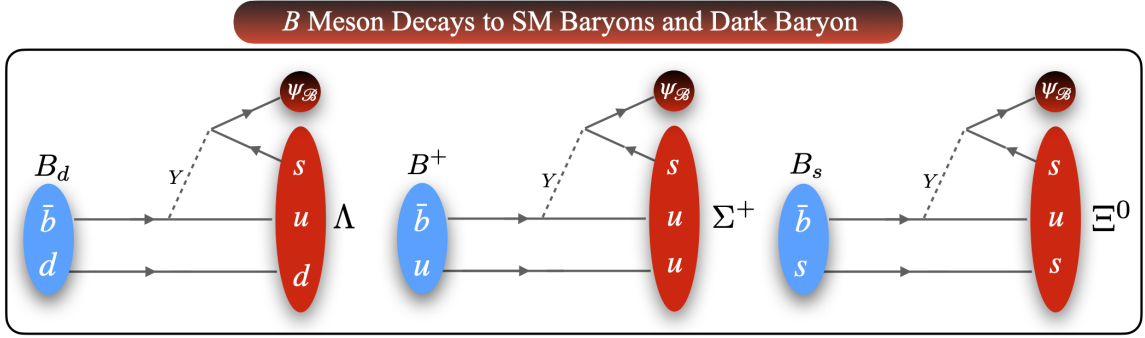


Figure 1. Decay modes of $B_{s,d}^0$ and B^+ mesons through the $\mathcal{O}_{b,us}$ and $\mathcal{O}_{s,ub}$ operators. Decays through the other operators listed in Table 1 arise in a similar way.

The *seemingly* baryon number violating decay of the charged or neutral B meson can generically proceed as follows: a colored scalar mediator⁴ Y can mediate the decay of a b -quark within the B meson to a SM baryon \mathcal{B}_{SM} and dark sector baryon $\psi_{\mathcal{B}}$ (which appears as missing energy in the detector). The Lagrangian for the model, allowed by all the symmetries, is

$$\mathcal{L} = -y_{u_\alpha d_\beta} \epsilon_{ijk} Y^{*i} \bar{u}_\alpha^j d_\beta^{c,k} - y_{\psi d_\gamma} Y_i \bar{\psi}_{\mathcal{B}} d_\gamma^{c,i} + \text{h.c.}, \quad (2.1)$$

where all SM quarks are right handed, and “c” indicates a charge conjugation. i, j, k are color indices, and α, β, γ are flavor indices. Here Y has the SM charge assignment $(3, 1, -1/3)$ ⁵. The colored mediator Y can be produced at the LHC and thus must have a mass at the TeV scale to be consistent with collider constraints [9]. Integrating out Y leads to the following effective operator at the low energies:

$$\mathcal{H}_{d_\gamma, u_\alpha d_\beta} = -\frac{y_{\psi d_\gamma} y_{u_\alpha d_\beta}}{M_Y^2} i \epsilon_{ijk} (\bar{\psi}_{\mathcal{B}} d_\gamma^{c,i}) (\bar{u}_\alpha^j d_\beta^{c,k}) + \text{h.c.}. \quad (2.2)$$

There are four different flavor combinations that correspond to operators that can mediate the decay of the b quark within the B^0 meson and thus contribute to the generated baryon asymmetry in the B -Mesogenesis framework. Each flavor combination can give rise to two possible effective operators:

$$\mathcal{O}_{b, u_\alpha d_\beta} \equiv i \epsilon_{ijk} b^i (\bar{d}_\beta^{c,j} u_\alpha^k) \quad \text{and} \quad \mathcal{O}_{d_\beta, u_\alpha b} \equiv i \epsilon_{ijk} d_\beta^i (\bar{b}^{c,j} u_\alpha^k) \quad (2.3)$$

where again the quarks are right handed and $u_\alpha = u, c$ and $d_\beta = d, s$; giving eight operators in total.

⁴ See [25] for a consistent UV realization of this theory where the heavy colored mediator is identified with a squark of a supersymmetric theory.

⁵Note that other charge assignments for the mediator are also possible e.g. $(3, 1, 2/3)$ or $(3, 2, -1/6)$ which lead to a variety of different flavor and collider constraints [9, 11]), and furthermore could allow the couplings of $\psi_{\mathcal{B}}$ to left handed quarks. For simplicity, we consider only the hypercharge $-1/3$ mediator case in the present work.

Flavorful Operator	Decay Channel	$F_R^{\mathcal{O}}, \tilde{F}_L^{\mathcal{O}}$ $\mathcal{O} = \mathcal{O}_{b,u_i d_j}$	$F_R^{\mathcal{O}}, \tilde{F}_L^{\mathcal{O}}$ $\mathcal{O} = \mathcal{O}_{d_k, u_i b}$	$\text{Br}(B \rightarrow \mathcal{B}_{\text{SM}} + \psi_{\mathcal{B}})$ $\mathcal{O} = \mathcal{O}_{b,u_i d_j}$	$\text{Br}(B \rightarrow \mathcal{B}_{\text{SM}} + \psi_{\mathcal{B}})$ $\mathcal{O} = \mathcal{O}_{d_k, u_i b}$
$\psi_{\mathcal{B}} b u d$	$B_d \rightarrow \psi_{\mathcal{B}} + n$	$R_1, 0$	$R_1, 0$	$3.7_{\pm 0.4} \cdot 10^{-7}$	$8.3_{\pm 0.9} \cdot 10^{-6}$
	$B_s \rightarrow \psi_{\mathcal{B}} + \Lambda$	n.a.	n.a.	n.a.	n.a.
	$B^+ \rightarrow \psi_{\mathcal{B}} + p$	R_2, \tilde{L}_1	$R_1, 0$	$9.6_{\pm 0.6} \cdot 10^{-8}$	$8.9_{\pm 0.9} \cdot 10^{-6}$
$\psi_{\mathcal{B}} b u s$	$B_d \rightarrow \psi_{\mathcal{B}} + \Lambda$	$R_1, 0$	$R_1, 0$	$1.2_{\pm 0.06} \cdot 10^{-5}$	$3.2_{\pm 0.6} \cdot 10^{-5}$
	$B_s \rightarrow \psi_{\mathcal{B}} + \Xi^0$	R_2, \tilde{L}_1	R_3, \tilde{L}_1	$2.6_{\pm 0.1} \cdot 10^{-6}$	$4.8_{\pm 0.2} \cdot 10^{-5}$
	$B^+ \rightarrow \psi_{\mathcal{B}} + \Sigma^+$	R_2, \tilde{L}_1	$R_1, 0$	$2.5_{\pm 0.3} \cdot 10^{-6}$	$2.1_{\pm 0.2} \cdot 10^{-5}$
$\psi_{\mathcal{B}} b c d$	$B_d \rightarrow \psi_{\mathcal{B}} + \Sigma_c^0$	R_2, \tilde{L}_1	R_3, \tilde{L}_1	$1.3_{\pm 0.6} \cdot 10^{-6}$	$2.7_{\pm 1.5} \cdot 10^{-4}$
	$B_s \rightarrow \psi_{\mathcal{B}} + \Xi_c^0$	R_2, \tilde{L}_1	R_3, \tilde{L}_1	$1.2_{\pm 0.6} \cdot 10^{-6}$	$2.3_{\pm 1.3} \cdot 10^{-4}$
	$B^+ \rightarrow \psi_{\mathcal{B}} + \Sigma_c^+$	R_2, \tilde{L}_1	R_3, \tilde{L}_1	$1.4_{\pm 0.7} \cdot 10^{-6}$	$2.9_{\pm 1.6} \cdot 10^{-4}$
$\psi_{\mathcal{B}} b c s$	$B_d \rightarrow \psi_{\mathcal{B}} + \Xi_c^0$	R_2, \tilde{L}_1	R_3, \tilde{L}_1	$8.4_{\pm 3.7} \cdot 10^{-6}$	$3.2_{\pm 1.7} \cdot 10^{-4}$
	$B_s \rightarrow \psi_{\mathcal{B}} + \Omega_c$	R_2, \tilde{L}_1	R_3, \tilde{L}_1	$9.0_{\pm 4.0} \cdot 10^{-6}$	$4.4_{\pm 2.0} \cdot 10^{-4}$
	$B^+ \rightarrow \psi_{\mathcal{B}} + \Xi_c^+$	R_2, \tilde{L}_1	R_3, \tilde{L}_1	$1.8_{\pm 0.6} \cdot 10^{-5}$	$3.5_{\pm 1.9} \cdot 10^{-4}$

Table 1. We summarize the possible B meson decay channels which can generate the baryon asymmetry in B -Mesogenesis. For each operator and decay mode we list the resulting structure of the form factor $R_{1,2,3}$ or \tilde{L}_1 given in Eqs. (3.3–3.6). In the final two columns we quote the maximum possible branching fraction for each operator. These are found by evaluating the branching fraction at $m_{\psi_{\mathcal{B}}} = 1$ GeV, and by fixing the Wilson coefficient to its maximum possible value allowed by LHC constraints, computed in [9]. Note that in the case of $B_d \rightarrow \psi_{\mathcal{B}} + \Sigma_c^0$, the very prompt decay $\Sigma_c^0 \rightarrow \Lambda_c^+ + \pi^-$ will result in additional subtitles for experimental reconstruction.

In Table 1 we list the four possible flavorful variations of the operator in Eq. (2.3) along with the corresponding B meson decay modes, through which the baryon asymmetry can be generated can proceed. Note that the model also allows the decay of B^+ mesons which, while not directly responsible for the generated baryon asymmetry, serves as an indirect probe of the mechanism. In Figure 1 we show the decays through the $\mathcal{O}_{b,us}/\mathcal{O}_{s,ub}$ operator for the $B_{s,d}^0$ meson as well as the B^+ meson. Note that the coefficients $y_{\psi d_\gamma} y_{u_\alpha d_\beta}/M_Y^2$ associated with the above operators are constrained by a combination of LHC searches and flavor observables (see [9] for a detailed analysis). For simplicity, where obvious, we will omit the flavor indices on the Wilson coefficient and use refer to it as y^2/M_Y^2 .

Paramount to confirming Mesogenesis as the mechanism by which Nature chose to generate the baryon asymmetry is the measurement of the various decay modes in Table 1. This is the main result of the present work.

Some final comments on the parameter space are now in order. The mass of the dark baryon $\psi_{\mathcal{B}}$, and thus the corresponding missing energy, is required to be within a window of roughly 1-4 GeV. The reason is as follows: First it must be the case that $m_{\psi_{\mathcal{B}}} < m_B - m_p \simeq 4.34$ GeV, such that the requisite decay of the B meson is kinematically allowed. Second, since the operator Eq. (2.2) can lead to proton decay, we simply require that any dark sector state charged under baryon number be sufficiently heavy to kinematically forbid

such decays and therefore stabilize matter⁶: $m_{\psi_B} > m_p - m_e \simeq 937.8\text{MeV}$. In summary, the dark baryon should have a mass in the range

$$m_p - m_e < m_{\psi_B} < m_B - m_{\mathcal{B}_{SM}}, \quad (2.4)$$

corresponding to a range about 1-4 GeV.

Finally, note that ψ_B cannot be the dark matter as it is unstable. Indeed, the operators of Eq. (2.2) would allow the decay $\psi_B \rightarrow p + e + \bar{\nu}_e$ which is kinematically allowed, and would washout the generated asymmetry. To evade washout and stabilize the dark matter additional dark sector states must be introduced. The dark sector dynamics has no implications on the current work and we simply refer the interested reader to [4, 6] for more details.

3 Form Factors from Light Cone Sum Rules

Historically, the LCSR technique was developed to explain the mass difference between the Σ -hyperion and the proton in the weak decay $\Sigma \rightarrow p + \gamma$ [19]. Technically, LCSR combines the QCD sum rules technique with the theory of hard exclusive processes. Intuitively, the short distance expansion is replaced by the expansion in the transverse distance between partons in light-cone coordinates [27]. This allows one to incorporate additional information about QCD correlators related to the approximate conformal symmetry of the theory. The order of the expansion is regulated by the *twist* of the operators [28, 29]. Twist is defined as the difference between the dimension and the spin of an operator; increasing the twist accuracy takes into account higher transverse momentum and higher Fock state contributions [30].

To compute the branching fractions of the two body meson to baryon decays listed in Table 1 via the QCD LCSR technique, one introduces a baryon to vacuum correlator. This object depends on the specific meson interpolating current and on the effective three-quark operator coupled to ψ_B . In the recent paper [31]⁷ the two body decay $B^+ \rightarrow p + \psi_B$ was obtained using the LCSR method. Our approach reproduces the result of [31], and we further generalize it to all the remaining decays that could contribute to the production of the baryon asymmetry. Unless explicitly stated otherwise, we will mostly refer to the B -meson triplet, (B_d, B_s, B^+) , without specifying the quark content, simply as B . A brief summary of the formalism is given in Appendix A.1, and we extended it to heavy baryons in Appendix A.2.

The two body decay amplitudes of interest all have the form:

$$\mathcal{A}(B \rightarrow \mathcal{B}_{SM} + \psi_B) = \frac{y_{\psi d_\gamma} y_{u_\alpha d_\beta}}{M_Y^2} \langle \mathcal{B}_{SM}(P) | \mathcal{O} | B(P+q) \rangle u_{\psi_B}^c(q), \quad (3.1)$$

where $u_{\psi_B}^c$ is the charge conjugated bispinor of the ψ_B field. Here $P+q$ and P are the momenta of the B -meson and \mathcal{B}_{SM} respectively while $y_{\psi d_\gamma} y_{u_\alpha d_\beta} / M_Y^2$ is the Wilson coefficient associated with the specific operator \mathcal{O} defined in Eq. (2.2). Lorentz covariance

⁶Neutron star bounds may place slightly more stringent constraints on the mass of dark baryons (see [26]) but these are model dependent so we can allow ourselves to be more relaxed.

⁷[31] appeared while the present work was being prepared.

dictates that the hadronic matrix element in Eq. (3.1) can be parameterized in terms of four independent form factors as follows:

$$\langle \mathcal{B}_{SM}(P) | \mathcal{O} | B(P+q) \rangle = F_R^{\mathcal{O}}(q^2) \bar{u}_{\mathcal{B}_R} + F_L^{\mathcal{O}}(q^2) \bar{u}_{\mathcal{B}_L} + \tilde{F}_R^{\mathcal{O}}(q^2) \frac{\not{q}}{m_{\mathcal{B}_{SM}}} \bar{u}_{\mathcal{B}_R} + \tilde{F}_L^{\mathcal{O}}(q^2) \frac{\not{q}}{m_{\mathcal{B}_{SM}}} \bar{u}_{\mathcal{B}_L}, \quad (3.2)$$

where $\bar{u}_{\mathcal{B}_{R,L}}$ is the chiral spinor associated with the baryon. The calculation of the various F_I 's appearing in Eq. (3.2) is analogous to the ones discussed in [31], and we refer the interested reader to the details in Appendix A.1. Of these four possible structures only two are found to be non-zero for the specific choice of transition operators we consider, namely, F_R and \tilde{F}_L — a consequence of taking only R -handed fields in Eq. (2.3). The different flavor structures produce three distinct forms of F_R and a single form \tilde{F}_L . All the transitions in Table 1 are calculated using the leading twist-3 DAs:

$$R_1(q^2) = \frac{m_b^3}{4m_B^2 f_B} \int_0^{\alpha_0^B} d\alpha e^{(m_B^2 - s(\alpha))/M^2} \left\{ \frac{\tilde{V}(\alpha)}{(1-\alpha)^2} \left(1 + \frac{(1-\alpha)^2 m_{\mathcal{B}_{SM}}^2 - q^2}{m_b^2} \right) \right\}, \quad (3.3)$$

$$R_2(q^2) = \frac{m_b m_{\mathcal{B}_{SM}}^2}{4m_B^2 f_B} \int_0^{\alpha_0^B} d\alpha e^{(m_B^2 - s(\alpha))/M^2} \left(\tilde{V}(\alpha) - 3 \frac{m_b}{m_{\mathcal{B}_{SM}}} \frac{\tilde{T}(\alpha)}{(1-\alpha)} \right), \quad (3.4)$$

$$R_3(q^2) = \frac{m_b^3}{4m_B^2 f_B} \int_0^{\alpha_0^B} d\alpha e^{(m_B^2 - s(\alpha))/M^2} \left\{ \left(1 - \frac{q^2}{m_b^2} \right) \frac{\tilde{V}(\alpha)}{(1-\alpha)^2} + 3 \frac{m_{\mathcal{B}_{SM}} \tilde{T}(\alpha)}{m_b (1-\alpha)} \right\}, \quad (3.5)$$

$$\tilde{L}_1(q^2) = \frac{m_b m_{\mathcal{B}_{SM}}^2}{4m_B^2 f_B} \int_0^{\alpha_0^B} d\alpha \frac{\tilde{V}(\alpha)}{(1-\alpha)} e^{(m_B^2 - s(\alpha))/M^2}. \quad (3.6)$$

Where in Eqs. (3.3–3.6) $s(\alpha) = [m_b^2 - \alpha q^2 + \alpha(1-\alpha)m_{\mathcal{B}_{SM}}^2]/(1-\alpha)$, and

$$\alpha_0^B = \frac{s_0^B - q^2 + m_{\mathcal{B}_{SM}}^2 - \sqrt{(s_0^B - q^2 + m_{\mathcal{B}_{SM}}^2)^2 - 4m_{\mathcal{B}_{SM}}^2 (s_0^B - m_b^2)}}{2m_{\mathcal{B}_{SM}}^2}. \quad (3.7)$$

Here s_0^B and M^2 are the effective threshold and the Borel parameter respectively. They correspond to “internal” parameters of the LCSR description that are to be fixed. The two functions appearing in the definitions of the sum rules above are the, once integrated, leading twist-3 DAs of for the specific baryon, given by [24]:

$$\tilde{V}(\alpha) = \int_0^{1-\alpha} d\alpha_2 [V_1 + A_1](\alpha, \alpha_2, 1 - \alpha - \alpha_2), \quad (3.8)$$

$$\tilde{T}(\alpha) = \int_0^{1-\alpha} d\alpha_2 T_1(\alpha, \alpha_2, 1 - \alpha - \alpha_2), \quad (3.9)$$

The functions V_1 , A_1 and T_1 are defined in Eqs. (1-9) of [24] or in Eqs. (6-9) of [32]. The definitions of the sum rules for charmed operators are not modified however subtleties are involved in the DAs of heavy-baryons; a dedicated discussion is given in A.2. From Eqs. (3.1–3.2) one can recover a convenient expression for the two-body branching ratio

mediated by a single operator:

$$\begin{aligned} \text{Br}(B \rightarrow \mathcal{B}_{\text{SM}} + \psi_{\mathcal{B}}) = & \frac{|y_{\psi d_\gamma} y_{u_\alpha d_\beta}|^2 \tau_B}{32\pi m_B^3 M_Y^4} \left\{ \left| R_I(m_{\psi_{\mathcal{B}}}^2) + \frac{m_{\psi_{\mathcal{B}}}}{m_{\mathcal{B}_{\text{SM}}}} \tilde{L}_I(m_{\psi_{\mathcal{B}}}^2) \right|^2 (m_B^2 - (m_{\mathcal{B}_{\text{SM}}} - m_{\psi_{\mathcal{B}}})^2) \right. \\ & \left. + \left| R_I(m_{\psi_{\mathcal{B}}}^2) - \frac{m_{\psi_{\mathcal{B}}}}{m_{\mathcal{B}_{\text{SM}}}} \tilde{L}_I(m_{\psi_{\mathcal{B}}}^2) \right|^2 (m_B^2 - (m_{\mathcal{B}_{\text{SM}}} + m_{\psi_{\mathcal{B}}})^2) \right\} \lambda^{1/2}(m_B^2, m_{\mathcal{B}_{\text{SM}}}^2, m_{\psi_{\mathcal{B}}}^2), \end{aligned} \quad (3.10)$$

where λ is the Källén function. The appropriate R_I and \tilde{L}_I can be read off the corresponding entry in Table 1.

4 Results

In this work we have used LCSRs to compute the exclusive branching fractions for each decay mode in Table 1 that could generate the baryon asymmetry in the Mesogenesis framework. Our results for the *maximum possible branching fraction* (in light of LHC constraints) are presented in Figure 2 and Figure 3 for B meson decays to light and heavy (charmed) baryons respectively. In what follows we will discuss some interesting features of these results, before moving on to comment on implications for testing B -Mesogenesis.

4.1 Discussion of Results

By substituting the results obtained in Appendix A.3 for the form factors⁸ into Eq. (3.10), we obtain the exclusive branching for all processes shown in Table 1. In Figure 2 the results for the maximum branching fraction from the first two flavorful operators, corresponding to decays of the B meson to lighter baryons, are shown as a function of $m_{\psi_{\mathcal{B}}}$. The plots are ordered with $\mathcal{O}_{b,u_i d_j}$ on the left and $\mathcal{O}_{d_k, u_i b}$ on the right. The first row corresponds to the operator $\psi_{\mathcal{B}} b u d$, while the second to $\psi_{\mathcal{B}} b u s$, mimicking the order of the top two rows of Table 1. LHC searches for new colored particles limit the size of the Wilson coefficient $(y/M_Y)^2$ for each operator — these bounds were computed in [9]. We fix $(y/M_Y)_{\text{max}}^2$ so that the plotted branching fractions represent the maximum possible ones. To obtain a branching ratio independent on the Wilson coefficient one can simply re-scale the curves by a factor of $1/(y/M_Y)^4$. In Figure 3 we present the maximum branching fractions (again using LHC bounds on the specific operators) for decays to charmed baryons mediated by the operators $\psi_{\mathcal{B}} b c d$, and $\psi_{\mathcal{B}} b c s$ i.e. the two bottom rows of Table 1. These branching fractions have been computed using the DAs from HQET by employing heavy-quark symmetry⁹. The maximal values of $(y/M_Y)_{\text{max}}^2$ are reported in each panel of Figure 2 and Figure 3. These are also used to compute the branching fractions values at $m_{\psi_{\mathcal{B}}} = 1$ GeV which are presented in the two right most columns of Table 1. These entries represent the overall maximum possible branching fractions and are important for understanding the implications for Mesogenesis, as we will discuss further below.

⁸In the following we will not explicitly distinguish form factors from their fits with the BCL expansion. The reader should keep in mind that any numerical results will be obtained via the values of the fits.

⁹A detailed discussion on charmed DAs can be found in Appendix A.2.

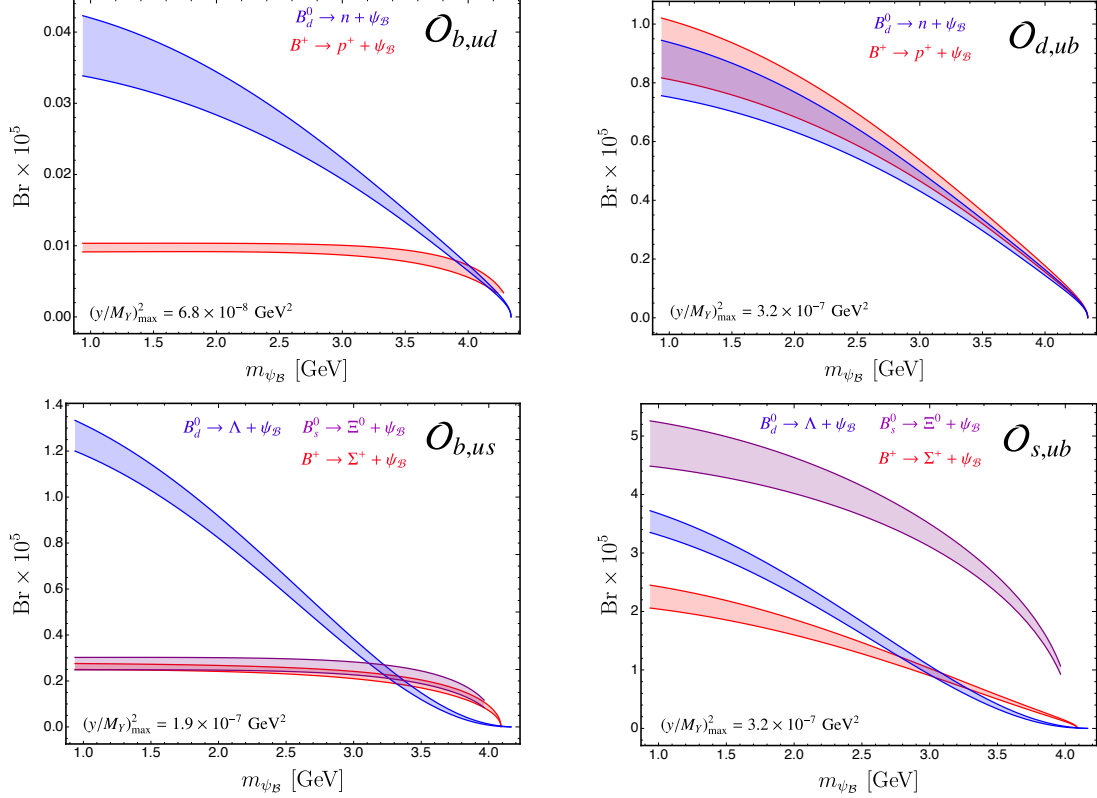


Figure 2. Branching fractions as a function of ψ_B mass for the decays arising from the light quark operators $\psi_B bud$ and $\psi_B bus$; the top two rows of Table 1. For each operator, we have fixed the Wilson coefficient to the maximum possible value allowed by LHC constraints, computed in [9]. The error bands come primarily from the uncertainties in the DAs and the errors on the internal parameters, as discussed in the text.

We can already learn a lot by considering the first operator $\psi_B bud$. For example it is interesting to see that $SU(2)_F$ violating effects are mainly due to the masses entering in the branching ratio formula Eq. (3.10), as the form factors are not really affected by these differences (see Table 3). This can be seen in the fifth column of Table 1 as the entries for the B_d and B^+ decay differ more than their respective form factors values. A second emerging pattern is the sub-dominance of the R_2 and \tilde{L}_1 structures in comparison to R_1 and R_3 . This effect is seen in all the transitions except $B_d \rightarrow \psi_B + n$. This suppression is simply due to the fact that the prefactors in Eq. (3.3) and (3.5) are a factor of $(m_b/m_{B_{SM}})^2$ larger than Eq. (3.4) and (3.6). The effect is even more pronounced in the heavy-baryon sector at small ψ_B masses as the contribution of \tilde{L}_1 receives an extra suppression factor of $m_{\psi_B}/m_{B_{SM}}$. Therefore at higher values of m_{ψ_B} it is possible to see a small enhancement in the decays mediated by $\mathcal{O}_{b,u_i d_k}$. In general the $\mathcal{O}_{d_k, u_i b}$ operators will give the higher contribution among the two.

Another notable feature in Table 1 is that the $B_s \rightarrow \psi_B + \Lambda$ transition appears to be prohibited at leading twist. The vanishing of the amplitude does not depend on the particular operator in Eq. (2.3) nor on the particular chirality of its fields. This selection

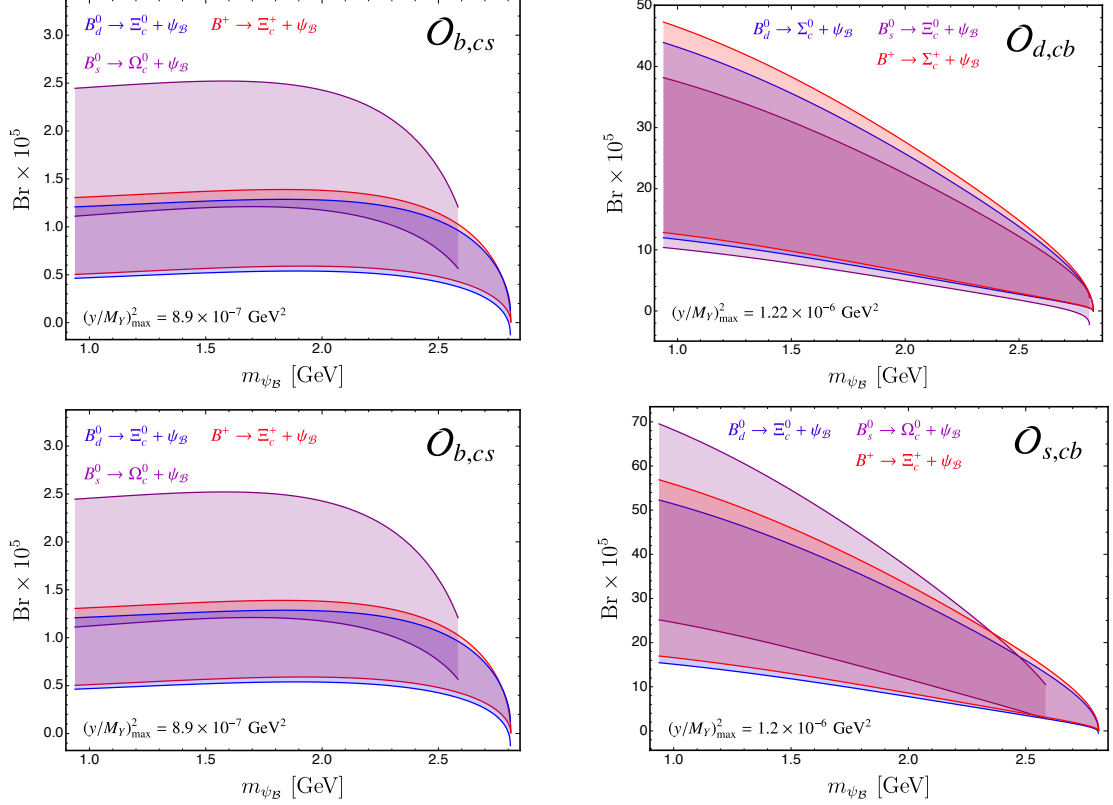


Figure 3. Branching fractions for decays from the charmed operators $\psi_{\mathcal{B}}bcd$ and $\psi_{\mathcal{B}}bcs$; the bottom two rows of Table 1. See App A.2 for a treatment of the DA for heavy quarks. For each operator, we have fixed the Wilson coefficient to the maximum possible value allowed by LHC constraints, computed in [9]. The larger uncertainties come from an additional 15% error that we apply on all parameters entering the DAs definition inferred by heavy-quark symmetry

rule is due to conservation of total angular momentum. The bounded di-quark system in the B_s meson will have total spin $j = 0$. In the final state the spinless di-quark system is given by the valence couple (u, d) while the spin of the baryon is carried solely by the spectator s -quark [24]. Therefore, conservation of total angular momentum imposes the spin of $\psi_{\mathcal{B}}$ to be opposite to the s quark spin; this is forbidden by the scalar nature of the operators studied in this work.

The maximum branching fractions for the heavier baryon final states in Figure 3 are typically an order of magnitude larger than the ones in Figure 2 simply due to the weaker LHC constraints on the charmed channels. The general features discussed for the first two operators still apply, e.g. the hierarchy between \mathcal{O}_{b,u_id_j} and \mathcal{O}_{d_k,u_ib} is still present.

Finally, the uncertainties appearing in Figure 2 are obtained by treating the internal parameters ranges as errors, (see App. A.3), and adding them in quadrature with the errors of the DAs parameters. In Figure 3, we note that the uncertainties are far more significant for the charmed baryon final states due to an additional 15% error that we apply on all parameters entering the DAs definition inferred by heavy-quark symmetry [33]. Otherwise, uncertainties are propagated in the same way as for decays to light baryons.

4.2 Implications for Mesogenesis

With the results for the branching fractions in hand, we now comment on the implications for testing Mesogenesis.

The Neutral B Mesogenesis [4] mechanism is currently the most testable of all the Mesogenesis scenarios. As such, for practical reasons alone, it is motivated for experimentalists to first focus on targeting its parameter space. As discussed above, successful Neutral B Mesogenesis requires an inclusive branching fraction that is greater than roughly $\text{Br}(B_{s,d}^0 \rightarrow \psi_{\mathcal{B}} + \mathcal{B}_{\text{SM}}) \gtrsim 10^{-5}$, in light of existing bounds on the CPV in the $B^0 - \bar{B}^0$ oscillation system. Several or all the $B_{s,d}^0$ decay modes listed in Table 1 could contribute to the generation of the asymmetry. Therefore, to *fully test* Neutral B Mesogenesis requires a *search for all possible decays*. To date one such search has been conducted; the Belle-II collaboration [17] performed a search targeting the decays through the $\psi_{\mathcal{B}} b u s$ operator, setting a limit $\text{Br}(B_d^0 \rightarrow \psi_{\mathcal{B}} + \Lambda) \lesssim 2 \times 10^{-5}$. Comparing this to the second row of Table 1 we see that this limit is *not* more constraining than the theoretical predictions for the branching fraction in light of LHC bounds on the Wilson coefficient. Furthermore, examining the maximum branching fractions in the first row of Table 1, we see that it is only marginally possible for $\psi_{\mathcal{B}} b u d$ operator to be entirely responsible for the generation of the baryon asymmetry. Meanwhile, the other three operators have branching fractions that could still be large enough to be entirely reasonable for the baryon asymmetry.

While Neutral B Mesogenesis is exceptionally testable on a short time scale, it is critical to emphasize that this not the only possible way to generate the baryon asymmetry by leveraging SM Meson systems. Other mechanisms of Mesogenesis involve the CPV in the decays of Charged D mesons [5], or B and B_c mesons [6]. In particular, for B_c Mesogenesis [6], the exact same model Eq. (2.1) is evoked to generate the baryon asymmetry. In this case, it is the branching fraction of the B^+ decays that directly feeds into the generated baryon asymmetry. From Fig 2 of [6], we can see that the branching fraction for $B^+ \rightarrow \psi_{\mathcal{B}} + \mathcal{B}_{\text{SM}}$ could be as small as 10^{-6} and still reasonably generate the baryon asymmetry. As such we conclude that every one of the operators in Table 1 is still a viable candidate for generating the asymmetry in this scenario.

Allowing for the most general scenario, the branching fraction could be as low as $\text{Br} \gtrsim 10^{-7}$ and still generate the baryon asymmetry, if all the CPV came entirely from the dark sector. This scenario is far less reconstructable but is nevertheless worth keeping in mind when conducting searches.

In summary, the branching fractions computed here provide experimentalists with a critical ingredient for testing Mesogenesis. Experiments such as Belle, BaBar, LHCb (and to some extent ATLAS and CMS) are primed to conduct searches for B mesons decaying into baryons and missing energy. Doing so could unveil the nature of baryogenesis and therefore our very existence.

5 Outlook

In this work we have presented the results of a LCSR calculation of the form factors and branching fractions for the seemingly baryon number violating decays of $B_{s,d}^0$ and B^+ mesons into a dark sector baryon ψ_B and various SM baryon final states. Figures 2 and 3 show the results for the maximum possible branching fractions (in light of LHC constraints on the Wilson coefficients) and associated uncertainties for each of the four flavorful variation on the operators that could produce the baryon asymmetry. These results will serve to guide experimental searches for these exclusive decay modes. Several interesting future directions exist, which we now comment briefly upon.

In the present work we considered operators involving only right handed fermions as would arise in the model defined by the Lagrangian in Eq. (2.1) i.e. where the colored mediator is a scalar and has SM hyper-charge assignment $-1/3$. However, other UV completions do exist corresponding to different charge assignments for the mediator (see the models in [9]). For instance, the mediator could be a doublet under $SU(2)_L$ which would give rise to four fermion operators containing left handed quarks. The branching fractions arising from these operators would lead to non-vanishing contributions from the $F_L^{\mathcal{O}}(q^2)$ and $\tilde{F}_R^{\mathcal{O}}(q^2)$ form factors. The computation of these form factors is a trivial extension and we leave it to future work.

The model of Eq. (2.1) would also give rise to the decay of a baryon into light mesons and missing energy e.g. $\Lambda_b \rightarrow \bar{\psi}_B + \pi^0$ through the $\mathcal{O}_{b,ud}$ and $\mathcal{O}_{d,ub}$ (see [4] for other decay modes). While the branching fraction of such decays do not directly feed into the Boltzmann equations that track the generated baryon asymmetry, they do serve as an indirect probe of B -Mesogenesis. Therefore, it would be interesting for experimental searches to target these decays as well. Indeed, the proposed search at LHCb [18] would be capable of measuring these b -flavored baryon decays. As such it is also a worthy peruse to also compute the predicted branching fractions for these decays. To do so one can once again use the LCSR machinery. The starting point would be a three point correlator and we leave the details of this interesting technical pursuit to future work.

Another application of the LCSR technique would to calculate the branching fractions of the B meson decay's in Table 1 where multiple final state light mesons are radiated e.g. π^0 .

Acknowledgments

We thank Zoltan Ligeti and Stefano Rigolin for useful conversations. G.E. is supported by the Cluster of Excellence *Precision Physics, Fundamental Interactions and Structure of Matter* (PRISMA⁺ – EXC 2118/1) within the German Excellence Strategy (project ID 39083149). A.W.M.G. is supported by the European Union's Horizon 2020 research and innovation programme under the Marie Skłodowska-Curie grant agreement 860881 (HIDDEN).

A Technical Details

We now give an overview of some of the more technical details of our derivation using the LCSR, the DAs for decays to heavy charmed final state baryons, and finally numerical results for extracting form factors.

A.1 Form Factors from LCSR

The central object of this approach is the correlation function mediating the $B \rightarrow \mathcal{B}_{\text{SM}} + \psi_{\mathcal{B}}$ transition:

$$\Pi(P, q) = i \int d^4x e^{i(P+q)\cdot x} \langle 0 | T \{ j_B(x), \mathcal{O}(0) \} | \mathcal{B}_{\text{SM}} \rangle, \quad (\text{A.1})$$

where $j_B = m_b \bar{b} i \gamma^5 u$ is the B meson interpolating current carrying four-momentum $(P+q)$, P and q are the \mathcal{B} and $\psi_{\mathcal{B}}$ momenta respectively while \mathcal{O} is one of the operators defined in Eqs. (2.3). The correlation function in Eq. (A.1) can be rewritten by employing an hadronic dispersion relation in the $(P+q)^2$ variable with the B -meson pole isolated

$$\Pi(P, q) = \frac{m_B^2 f_B \langle B(P+q) | \mathcal{O} | \mathcal{B}_{\text{SM}}(P) \rangle}{m_B^2 - (P+q)^2} + \int_{s_h}^{\infty} ds \frac{\rho(s, q^2)}{s - (P+q)^2}, \quad (\text{A.2})$$

where we used the identity $\langle 0 | j_B | B \rangle = m_B^2 f_B$. Here ρ is the spectral density encapsulating contributions from the excited and continuum states above threshold. $\Pi(P, q)$ can be decomposed in terms of Lorentz covariant structures:

$$\begin{aligned} \Pi(P, q) = & \Pi_R((P+q)^2, q^2) \bar{u}_{\mathcal{B}_R} + \Pi_L((P+q)^2, q^2) \bar{u}_{\mathcal{B}_L} \\ & + \tilde{\Pi}_R((P+q)^2, q^2) \not{q} \bar{u}_{\mathcal{B}_R} + \tilde{\Pi}_L((P+q)^2, q^2) \not{q} \bar{u}_{\mathcal{B}_L}, \end{aligned} \quad (\text{A.3})$$

where the $\Pi_{L,R}, \tilde{\Pi}_{L,R}$ are Lorentz invariant functions. Substituting Eq. (3.2) and Eq. (A.3) in Eq. (A.2) exposes the form factors in the hadronic matrix element in terms of the Lorentz invariant Π_I ¹⁰ functions, namely

$$\Pi_I((P+q)^2, q^2) = \frac{m_B^2 f_B F_I(q^2)}{m_B^2 - (P+q)^2} + \int_{s_h}^{\infty} ds \frac{\rho_I(s, q^2)}{s - (P+q)^2}. \quad (\text{A.4})$$

Note that to compute $\Pi_I = \tilde{\Pi}_{R,L}$ requires the substitution $F_I \rightarrow m_{\mathcal{B}_{\text{SM}}}^{-1} \tilde{F}_{R,L}$. In the region where the momenta are very far off-shell, $(P+q)^2, q^2 \ll m_b^2$, the integral Eq. (A.1) is dominated by modes near the light-cone $x^2 = 0$. In this case the computation is carried out via a light-cone OPE convoluted with the distribution amplitudes (DAs) of the baryons [24], we refer to the correlation function computed in this way as Π_I^{OPE} . The invariant amplitudes calculated in this way can be written with a convenient dispersion relations, i.e.

$$\Pi_I^{\text{OPE}}((P+q)^2, q^2) = \frac{1}{\pi} \int_{m_b^2}^{\infty} ds \frac{\text{Im}\{\Pi_I^{\text{OPE}}(s, q^2)\}}{s - (P+q)^2}. \quad (\text{A.5})$$

Substituting Eq. (A.5) and evoking semi-global quark hadron duality we have

$$\int_{s_h}^{\infty} ds \frac{\rho_I(s, q^2)}{s - (P+q)^2} = \frac{1}{\pi} \int_{s_0^B}^{\infty} ds \frac{\text{Im}\{\Pi_I^{\text{OPE}}(s, q^2)\}}{s - (P+q)^2}, \quad (\text{A.6})$$

¹⁰The superindex I is intended to include $\Pi_{L,R}$ and $\tilde{\Pi}_{L,R}$.

in Eq. (A.4). We then take the standard Borel transformation, $(P + q)^2 \rightarrow M^2$, to obtain the LCSR master formula for the form factors:

$$m_B^2 f_B F_I(q^2) e^{-m_B^2/M^2} = \frac{1}{\pi} \int_{m_b^2}^{s_0^B} ds e^{-s/M^2} \text{Im}\{\Pi_I^{\text{OPE}}(s, q^2)\}, \quad (\text{A.7})$$

where s_0^B is the effective threshold. Once again, whenever one wishes to consider $\Pi_I = \tilde{\Pi}_{R,L}$ the correct substitution for the form factor is simply $F_I \rightarrow m_{\mathcal{B}_{\text{SM}}}^{-1} \tilde{F}_{R,L}$. Now, to derive Eqs. (3.3–3.6) from Eq. (A.7) one simply has to revert back to the original integration variable α , and substitute the invariant amplitude calculated at leading twist in the OPE. Note that whenever the momentum combination $(P + q)^2$ appears in the numerator of the invariant amplitudes one has to remove it via a subtraction of a term independent of $(P + q)^2$. These can then be omitted as they vanish after the Borel transformation.

A.2 Charmed Sector Distribution Amplitudes

Since there are no Lattice QCD results for the DAs beyond the baryon octet, one is forced to employ a model to tackle heavier states. To extend the analysis to charmed baryons one can employ the DAs obtained in the HQET [34, 35] and assume heavy quark symmetry [36]. The only resonances participating in the decays of Table 1 are of the $SU(3)_F$ anti-triplet and sextet with spin parity $J^P = 1/2^+$. Let us first consider the anti-triplet states, characterized by $j^P = 0^+$ for the light di-quark system¹¹, these can be decomposed at leading twist as

$$\langle 0 | q_{1\alpha}(t_1) q_{2\beta}(t_2) Q_\gamma(0) | H_Q^{j=0} \rangle = \left(\sum_i B_i^{j=0} [\Gamma_i C^{-1}]_{\alpha\beta} \right) (u_{H_Q})_\gamma, \quad (\text{A.8})$$

where the basis is defined as $\Gamma_1 = \gamma^5 \not{n}$, $\Gamma_2 = 1/2 \sigma_{\bar{n}n} \gamma^5$, $\Gamma_3 = \gamma^5$ and $\Gamma_4 = \gamma^5 \not{n}$, and $(u_{H_Q})_\gamma$ is the spinor associated to the heavy baryon. Here n_μ is the light cone vector along which the light-quarks are aligned, \bar{n}_μ is its orthogonal direction and $\sigma_{\bar{n}n} = \sigma_{\mu\nu} \bar{n}^\mu n^\nu$. To find the coefficients of the decomposition, one imposes Eq. (23) of Ref. [35]. At leading-twist only $B_1^{j=0}$ is non-zero,

$$B_1^{j=0} = \frac{1}{8} v^+ \psi^2(t_1, t_2) f_{H_Q^{j=0}}, \quad (\text{A.9})$$

where v^+ is the projection of the velocity of the heavy quark Q_γ along the n_μ direction. ψ^2 and $f_{H_Q^{j=0}}$ are defined in [35]. In the $j = 1^+$ case a similar decomposition holds [37] with the substitutions $\Gamma_1 = \not{n}$, $(u_{H_Q})_\gamma \rightarrow (\gamma^5 u_{H_Q})_\gamma$, and

$$B_1^{j=1} = \frac{1}{8v^+} \psi^2(t_1, t_2) f_{H_Q^{j=1}}. \quad (\text{A.10})$$

Now one can connect the DAs in [35] with the ones defined in [24]. One can see that, in the $j = 0$, case the equality connecting the two definitions is

$$\frac{f_{H_Q^{j=0}}}{M_Q} \psi^2(x, 0) = \mathcal{A}(x, 0, 0), \quad (\text{A.11})$$

¹¹ j is the spin of the valence light quark couple.

Parameter	Numerics
Renormalization scale	$\mu = 3 \text{ GeV}$
Effective threshold	$s_0^B = 39 \pm 1.25 \text{ GeV}^2$
Borel Parameter Squared	$M^2 = 16 \pm 4 \text{ GeV}^2$

Table 2. Values and intervals of the internal parameters.

this can be proved by noting that $M_Q v^+ \not{v} = \not{\tilde{h}}$, where $\not{\tilde{h}}$ is defined in Eq. (4) of Ref. [24]. For practical reasons it is useful to find an identity between the Fourier transformed of the two i.e.

$$\begin{aligned} \int d\alpha_1 d\alpha_2 e^{-iP \cdot x \alpha_1} \delta\left(\frac{M_Q - m_Q}{M_Q} - \alpha_1 - \alpha_2\right) A\left(\alpha_1, \alpha_2, \frac{m_Q}{M_Q}\right) \\ = \int d\alpha'_1 d\alpha'_2 e^{-iP \cdot x \alpha'_1} \delta(1 - \alpha'_1 - \alpha'_2) \phi(\alpha'_1, \alpha'_2), \end{aligned} \quad (\text{A.12})$$

where M_Q and m_Q are the masses of the baryon and the heavy quark respectively and ϕ is defined as

$$\phi(\alpha_1, \alpha_2) = f_{H_Q^j} M_Q^3 \left(1 - \frac{m_Q}{M_Q}\right)^4 \left[\alpha_1 \alpha_2 \sum_{n=0}^2 \frac{a_n C_n^{3/2}(\alpha_1 - \alpha_2)}{\epsilon_n^4 |C_n^{3/2}|} e^{-(M_Q - m_Q)/\epsilon_n} \right]. \quad (\text{A.13})$$

The function \mathcal{A} is defined as as

$$\mathcal{A}(x, 0, 0) = \int d\alpha_1 d\alpha_2 d\alpha_3 \delta(1 - \sum_i \alpha_i) e^{-iP \cdot x \alpha_1} A(\alpha_1, \alpha_2, \alpha_3), \quad (\text{A.14})$$

and the HQET hypothesis introduces the constraint $\delta(\alpha_3 - m_Q/M_Q)$ in Eq. (A.12). A similar argument can be used for the $j = 1$ case, see [37], by swapping A for the V function. These DAs for charmed baryons can then be substituted in the results of Eqs. (3.3–3.6) and, after the fit discussed in App. A.3, will produce the results of Figure 3.

A.3 BCL Fits and Parameters

Here we will first discuss the values of the parameters we used to obtain the results of Sec. 4, we then present the details regarding the fit of the form factors in the kinematically allowed region.

The DAs are taken from the latest Lattice QCD results for the octet baryons [24], while the HQET Light-Cone DAs can be found in [35]. Finally the wave function normalizations at the origin for the charmed baryons are then taken from [38–40]. DAs are expanded in terms of orthogonal polynomials in such a way that the one loop scale dependence of their coefficients is autonomous (conformal partial wave expansion). In this way the non-perturbative information is encoded in scale dependent coefficients known as *shape parameters*. The running effects for the shape parameters and the couplings are taken into account using the results in [32, 41]. The Borel parameter M^2 and the renormalization scale μ are taken in the optimal ranges for a correlation function with the B -meson interpolation

Decay Channels	Fit Parameters	R_I^b	$R_I^{d_k}$	\tilde{L}_1
$B_d \rightarrow \psi_B + n$	$F_I(0)$	$1.94_{\pm 0.12} \cdot 10^{-2}$	$1.94_{\pm 0.12} \cdot 10^{-2}$	n.a.
	b_I	$3.07_{0.17}^{0.11}$	$3.07_{0.17}^{0.11}$	n.a.
$B_s \rightarrow \psi_B + \Lambda$	$F_I(0)$	n.a.	n.a.	n.a.
	b_I	n.a.	n.a.	n.a.
$B^+ \rightarrow \psi_B + p$	$F_I(0)$	$-9.20_{\pm 0.29} \cdot 10^{-3}$	$1.94_{\pm 0.11} \cdot 10^{-2}$	$5.87_{\pm 0.29} \cdot 10^{-4}$
	b_I	$-1.48_{0.21}^{0.22}$	$3.07_{0.17}^{0.11}$	$-2.83_{0.29}^{0.26}$
$B_d \rightarrow \psi_B + \Lambda$	$F_I(0)$	$4.09_{\pm 0.11} \cdot 10^{-2}$	$4.09_{\pm 0.11} \cdot 10^{-2}$	n.a.
	b_I	$6.91_{0.18}^{0.18}$	$6.91_{0.18}^{0.18}$	n.a.
$B_s \rightarrow \psi_B + \Xi^0$	$F_I(0)$	$-1.83_{\pm 0.09} \cdot 10^{-2}$	$4.69_{\pm 0.19} \cdot 10^{-2}$	$9.54_{\pm 0.65} \cdot 10^{-4}$
	b_I	$-1.83_{-0.04}^{-0.17}$	$1.57_{0.25}^{0.23}$	$-3.17_{0.45}^{0.39}$
$B^+ \rightarrow \psi_B + \Sigma^+$	$F_I(0)$	$-1.73_{\pm 0.04} \cdot 10^{-2}$	$3.12_{\pm 0.14} \cdot 10^{-2}$	$9.29_{\pm 0.54} \cdot 10^{-4}$
	b_I	$-1.07_{-0.11}^{-0.12}$	$4.63_{-0.02}^{-0.02}$	$-3.00_{0.32}^{0.29}$
$B_d \rightarrow \psi_B + \Sigma_c^0$	$F_I(0)$	$7.19_{\pm 1.8} \cdot 10^{-3}$	$3.76_{\pm 1.1} \cdot 10^{-2}$	$8.94_{\pm 2.3} \cdot 10^{-3}$
	b_I	$2.49_{-1.50}^{-0.91}$	$13.0_{-3.2}^{-1.8}$	$1.61_{-2.0}^{-1.2}$
$B_s \rightarrow \psi_B + \Xi_c^0$	$F_I(0)$	$6.92_{\pm 1.7} \cdot 10^{-3}$	$3.53_{\pm 0.94} \cdot 10^{-2}$	$8.56_{\pm 2.2} \cdot 10^{-3}$
	b_I	$2.70_{-1.40}^{-0.89}$	$13.5_{-3.1}^{-1.8}$	$1.81_{-1.9}^{-1.2}$
$B^+ \rightarrow \psi_B + \Sigma_c^+$	$F_I(0)$	$7.18_{\pm 1.80} \cdot 10^{-3}$	$3.76_{\pm 1.10} \cdot 10^{-2}$	$8.94_{\pm 2.30} \cdot 10^{-3}$
	b_I	$2.51_{-1.50}^{-0.92}$	$13.0_{-3.2}^{-1.8}$	$1.63_{-2.00}^{-1.20}$
$B_d \rightarrow \psi_B + \Xi_c^0$	$F_I(0)$	$8.17_{\pm 1.90} \cdot 10^{-3}$	$4.16_{\pm 1.10} \cdot 10^{-2}$	$1.01_{\pm 0.25} \cdot 10^{-2}$
	b_I	$2.64_{-1.40}^{-0.85}$	$13.2_{-3.0}^{-1.7}$	$1.77_{-1.90}^{-1.10}$
$B_s \rightarrow \psi_B + \Omega_c$	$F_I(0)$	$1.24_{\pm 0.25} \cdot 10^{-2}$	$5.12_{\pm 1.20} \cdot 10^{-2}$	$1.51_{\pm 0.32} \cdot 10^{-2}$
	b_I	$3.90_{-1.56}^{-1.05}$	$16.5_{-3.30}^{-2.10}$	$3.33_{-2.07}^{-1.35}$
$B^+ \rightarrow \psi_B + \Xi_c^+$	$F_I(0)$	$8.17_{\pm 1.90} \cdot 10^{-3}$	$4.18_{\pm 1.11} \cdot 10^{-2}$	$1.01_{\pm 0.32} \cdot 10^{-2}$
	b_I	$2.61_{-1.37}^{-0.84}$	$13.2_{-2.9}^{-1.7}$	$1.73_{-2.70}^{-1.40}$

Table 3. Fit parameters for the different decay channels.

current [31, 42, 43]. The effective threshold s_0^B is then fixed by fitting the mass of the B -meson obtained from the logarithmic derivative of the sum rule with the measured one, at each value of M^2 , by allowing a variation of 3% [44, 45]. Masses and parameters of mesons and quarks are taken from [46], while the internal values used to reproduce the results are reported in Table 2.

The form factors in Eq. (3.3–3.6) are calculated for $q^2 \ll m_b^2$, including the spacelike region $q^2 < 0$. To extrapolate the result in the whole kinematic region it is customary to employ the z -expansion, this involves mapping q^2 to a new variable z defined as

$$z(q^2) = \frac{\sqrt{t_+ - q^2} - \sqrt{t_+ - t_0}}{\sqrt{t_+ - q^2} + \sqrt{t_+ - t_0}}, \quad (\text{A.15})$$

where $t_+ = (m_B + m_{\mathcal{B}_{\text{SM}}})^2$ and $t_0 = (m_B + m_{\mathcal{B}_{\text{SM}}})(\sqrt{m_B} - \sqrt{m_{\mathcal{B}_{\text{SM}}}})$. This change of variables maps the whole complex q^2 plane onto the unit disk in the z plane, with the

paths along the branch cut mapped on the circle enclosing the unit disk. Moreover the choice of t_0 makes it so that the kinematically allowed region is centered around the origin and limited by $|z| < 0.08$ for all the decays considered. We choose to fit our results onto the Bourely-Caprini-Lellouch (BCL) expansion [47] slightly modified according to [42],

$$F_I(q^2) = \frac{F_I(0)}{1 - q^2/m_{\Lambda_b}^2} \left\{ 1 + b_I \left[z(q^2) - z(0) + \frac{1}{2} (z(q^2)^2 - z(0)^2) \right] \right\}. \quad (\text{A.16})$$

We use the interval $-5.0 < q^2 < 1 \text{ GeV}^2$ to perform the fit. The uncertainties are obtained by varying the internal parameters in their range and adding them in quadrature with the errors on the shape parameters of the DAs. In the case of charmed baryons the violation of heavy quark symmetry is obtained by adding a flat 15% error [33] on the couplings and on the parameters of the DAs. A report on the two parameter fit for each operator and channel is included in Table 3. For each channel we report the values of $F_I(0)$ and b for the three possible form factors. In the first two columns R_I from \mathcal{O}_{b,u_i,d_j} and R_I from $\mathcal{O}_{d_k,u_i,b}$ are reported. They are dubbed R_I^b and R_I^{dk} respectively. Finally the last column is dedicated to \tilde{L}_1 . Note that \tilde{L}_1 does not depend on the operator.

The values reported in Table 3 define three distinct curves for each form factor of a single transition corresponding to the extremes of the region allowed by the errors and to its central value. The latter is recovered by substituting the entries reported in Table 3 in Eq.(A.16). The other two curves correspond to the values of the parameters $F_I^\pm(0) = F_I(0) \pm \delta(F_I(0))$ and $b_I^\pm = b_I + b_I^{\text{Sup}}$ and $b_I^- = b_I - b_{I\text{Sub}}$, where $\delta(F_I(0))$ is the error reported in Tab 3 while b_I^{Sup} and $b_{I\text{Sub}}$ are the superscript and subscript corresponding to the parameter b respectively.

References

- [1] **Planck** Collaboration, P. A. R. Ade et al., *Planck 2015 results. XIII. Cosmological parameters*, *Astron. Astrophys.* **594** (2016) A13, [[arXiv:1502.01589](#)].
- [2] **Planck** Collaboration, N. Aghanim et al., *Planck 2018 results. VI. Cosmological parameters*, *Astron. Astrophys.* **641** (2020) A6, [[arXiv:1807.06209](#)]. [Erratum: *Astron. Astrophys.* 652, C4 (2021)].
- [3] R. H. Cyburt, B. D. Fields, K. A. Olive, and T.-H. Yeh, *Big Bang Nucleosynthesis: 2015*, *Rev. Mod. Phys.* **88** (2016) 015004, [[arXiv:1505.01076](#)].
- [4] G. Elor, M. Escudero, and A. Nelson, *Baryogenesis and Dark Matter from B Mesons*, *Phys. Rev. D* **99** (2019), no. 3 035031, [[arXiv:1810.00880](#)].
- [5] G. Elor and R. McGehee, *Making the Universe at 20 MeV*, *Phys. Rev. D* **103** (2021), no. 3 035005, [[arXiv:2011.06115](#)].
- [6] F. Elahi, G. Elor, and R. McGehee, *Charged B mesogenesis*, *Phys. Rev. D* **105** (2022), no. 5 055024, [[arXiv:2109.09751](#)].
- [7] A. D. Sakharov, *Violation of CP Invariance, c Asymmetry, and Baryon Asymmetry of the Universe*, *Pisma Zh. Eksp. Teor. Fiz.* **5** (1967) 32–35. [*Usp. Fiz. Nauk*161,61(1991)].
- [8] G. Elor et al., *New Ideas in Baryogenesis: A Snowmass White Paper*, in *2022 Snowmass Summer Study*, 3, 2022. [arXiv:2203.05010](#).

- [9] G. Alonso-Álvarez, G. Elor, and M. Escudero, *Collider signals of baryogenesis and dark matter from B mesons: A roadmap to discovery*, *Phys. Rev. D* **104** (2021), no. 3 035028, [[arXiv:2101.02706](#)].
- [10] M. Borsato et al., *Unleashing the full power of LHCb to probe stealth new physics*, *Rept. Prog. Phys.* **85** (2022), no. 2 024201, [[arXiv:2105.12668](#)].
- [11] G. Alonso-Álvarez, G. Elor, M. Escudero, B. Fornal, B. Grinstein, and J. Martin Camalich, *Strange physics of dark baryons*, *Phys. Rev. D* **105** (2022), no. 11 115005, [[arXiv:2111.12712](#)].
- [12] E. Goudzovski et al., *New Physics Searches at Kaon and Hyperon Factories*, [arXiv:2201.07805](#).
- [13] J. Berger, G. Elor [To Appear](#).
- [14] P. Asadi et al., *Early-Universe Model Building*, [arXiv:2203.06680](#).
- [15] J. L. Barrow et al., *Theories and Experiments for Testable Baryogenesis Mechanisms: A Snowmass White Paper*, [arXiv:2203.07059](#).
- [16] P. J. Fox et al., *TF08 Snowmass Report: BSM Model Building*, [arXiv:2210.03075](#).
- [17] Belle Collaboration, C. Hadjivasiliou et al., *Search for B^0 meson decays into Λ and missing energy with a hadronic tagging method at Belle*, *Phys. Rev. D* **105** (2022), no. 5 L051101, [[arXiv:2110.14086](#)].
- [18] A. B. Rodriguez, V. Chobanova, X. Cid Vidal, S. L. Solino, D. M. Santos, T. Mombacher, C. Prouve, E. X. R. Fernandez, and C. Vazquez Sierra, *Prospects on searches for baryonic Dark Matter produced in b-hadron decays at LHCb*, *Eur. Phys. J. C* **81** (2021), no. 11 964, [[arXiv:2106.12870](#)].
- [19] I. Balitsky, V. Braun, and A. Kolesnichenko, *Radiative decay $\sigma^+ \rightarrow p\gamma$ in quantum chromodynamics*, *Nuclear Physics B* **312** (1989), no. 3 509–550.
- [20] V. M. Braun and I. E. Filyanov, *QCD Sum Rules in Exclusive Kinematics and Pion Wave Function*, *Z. Phys. C* **44** (1989) 157.
- [21] V. L. Chernyak and I. R. Zhitnitsky, *B meson exclusive decays into baryons*, *Nucl. Phys. B* **345** (1990) 137–172.
- [22] P. Colangelo and A. Khodjamirian, *QCD sum rules, a modern perspective*, [hep-ph/0010175](#).
- [23] G. Lepage and S. J. Brodsky, *Exclusive Processes in Perturbative Quantum Chromodynamics*, *Phys. Rev. D* **22** (1980) 2157.
- [24] RQCD Collaboration, G. S. Bali et al., *Light-cone distribution amplitudes of octet baryons from lattice QCD*, *Eur. Phys. J. A* **55** (2019), no. 7 116, [[arXiv:1903.12590](#)].
- [25] G. Alonso-Álvarez, G. Elor, A. E. Nelson, and H. Xiao, *A Supersymmetric Theory of Baryogenesis and Sterile Sneutrino Dark Matter from B Mesons*, *JHEP* **03** (2020) 046, [[arXiv:1907.10612](#)].
- [26] D. McKeen, A. E. Nelson, S. Reddy, and D. Zhou, *Neutron stars exclude light dark baryons*, *Phys. Rev. Lett.* **121** (2018), no. 6 061802, [[arXiv:1802.08244](#)].
- [27] V. M. Braun, *Light cone sum rules*, in *4th International Workshop on Progress in Heavy Quark Physics*, pp. 105–118, 9, 1997. [hep-ph/9801222](#).

- [28] T. Ohrndorf, *Constraints from conformal covariance on the mixing of operators of lowest twist*, *Nuclear Physics B* **198** (1982), no. 1 26–44.
- [29] V. M. Braun and I. E. Filyanov, *Conformal Invariance and Pion Wave Functions of Nonleading Twist*, *Z. Phys. C* **48** (1990) 239–248.
- [30] P. Ball and V. M. Braun, *Handbook of higher twist distribution amplitudes of vector mesons in QCD*, in *3rd Workshop on Continuous Advances in QCD (QCD 98)*, pp. 125–141, 4, 1998. [hep-ph/9808229](#).
- [31] A. Khodjamirian and M. Wald, *B-meson decay into a proton and dark antibaryon from QCD light-cone sum rules*, [arXiv:2206.11601](#).
- [32] I. V. Anikin, V. M. Braun, and N. Offen, *Nucleon Form Factors and Distribution Amplitudes in QCD*, *Phys. Rev. D* **88** (2013) 114021, [[arXiv:1310.1375](#)].
- [33] A. Khodjamirian, *Quark-flavor symmetries and their violation in quantum chromodynamics*, *Phys. Atom. Nucl.* **80** (2017), no. 3 542–548.
- [34] A. G. Grozin and M. Neubert, *Asymptotics of heavy-meson form factors*, *Phys. Rev. D* **55** (Jan, 1997) 272–290.
- [35] A. Ali, C. Hambrock, A. Y. Parkhomenko, and W. Wang, *Light-Cone Distribution Amplitudes of the Ground State Bottom Baryons in HQET*, *Eur. Phys. J. C* **73** (2013), no. 2 2302, [[arXiv:1212.3280](#)].
- [36] M. Neubert, *Heavy quark symmetry*, *Phys. Rept.* **245** (1994) 259–396, [[hep-ph/9306320](#)].
- [37] T. M. Aliev, M. Savci, and S. Bilmis, *Charmed baryon $\Omega_c^0 \rightarrow \Omega^- l^+ \nu_l$ and $\Omega_c^0 \rightarrow \Omega_c^- \pi^+ (\rho^+)$ decays in light cone sum rules*, [arXiv:2208.10365](#).
- [38] T. M. Aliev, K. Azizi, and H. Sundu, *Analysis of the structure of $\Xi(1690)$ through its decays*, *Eur. Phys. J. C* **78** (2018), no. 5 396, [[arXiv:1804.02656](#)].
- [39] S. Groote, J. G. Körner, and O. I. Yakovlev, *Analysis of diagonal and nondiagonal qcd sum rules for heavy baryons at next-to-leading order in α_S* , *Phys. Rev. D* **56** (Oct, 1997) 3943–3954.
- [40] S. S. Agaev, K. Azizi, and H. Sundu, *Interpretation of the new Ω_c^0 states via their mass and width*, *Eur. Phys. J. C* **77** (2017), no. 6 395, [[arXiv:1704.04928](#)].
- [41] P. Ball, V. M. Braun, and E. Gardi, *Distribution Amplitudes of the Lambda(b) Baryon in QCD*, *Phys. Lett. B* **665** (2008) 197–204, [[arXiv:0804.2424](#)].
- [42] A. Khodjamirian and A. V. Rusov, *$B_s \rightarrow K l \nu_\ell$ and $B_{(s)} \rightarrow \pi(K) \ell^+ \ell^-$ decays at large recoil and CKM matrix elements*, *JHEP* **08** (2017) 112, [[arXiv:1703.04765](#)].
- [43] A. Khodjamirian, B. Melić, Y.-M. Wang, and Y.-B. Wei, *The $D^* D \pi$ and $B^* B \pi$ couplings from light-cone sum rules*, *JHEP* **03** (2021) 016, [[arXiv:2011.11275](#)].
- [44] A. Khodjamirian, T. Mannel, N. Offen, and Y. M. Wang, *$B \rightarrow \pi l \nu_l$ Width and $|V_{ub}|$ from QCD Light-Cone Sum Rules*, *Phys. Rev. D* **83** (2011) 094031, [[arXiv:1103.2655](#)].
- [45] G. Duplancic, A. Khodjamirian, T. Mannel, B. Melic, and N. Offen, *Light-cone sum rules for $B \rightarrow \pi$ form factors revisited*, *JHEP* **04** (2008) 014, [[arXiv:0801.1796](#)].
- [46] **Particle Data Group** Collaboration, R. L. Workman and Others, *Review of Particle Physics*, *PTEP* **2022** (2022) 083C01.

- [47] C. Bourrely, I. Caprini, and L. Lellouch, *Model-independent description of $B \rightarrow \pi l \nu$ decays and a determination of $|V_{ub}|$* , *Phys. Rev. D* **79** (2009) 013008, [[arXiv:0807.2722](https://arxiv.org/abs/0807.2722)]. [Erratum: *Phys.Rev.D* 82, 099902 (2010)].